

Melting Point Equations for the Ternary System Water/Sodium Chloride/Ethylene Glycol Revisited

James D. Benson^a, Aniruddha Bagchi^b, Xu Han^c, John K. Critser^c, Erik J. Woods^{d,e,*}

^a*Mathematical and Computational Sciences Division, National Institute of Standards and Technology, Gaithersburg, MD, 20879*

^b*Department of Mechanical Engineering, University of Minnesota, Minneapolis, MN*
^c*Department of Veterinary Pathobiology, University of Missouri, Columbia, MO, 65211*

^d*General BioTechnology, LLC, Indianapolis, IN, USA*

^e*Indiana University School of Medicine, Indianapolis, IN, USA*

Abstract

Partial phase diagrams are of considerable utility in the development of optimized cryobiological procedures. Recent theoretical predictions of the melting points of ternary solutions of interest to cryobiology have caused us to re-examine measurements that our group made for the ethylene-glycol–sodium chloride–water phase diagram. Here we revisit our previous experiments by measuring melting points at five ethylene-glycol to sodium chloride ratios (R values; $R = 5, 10, 15, 30,$ and 45) and five levels of concentration for each ratio. Melting points were averaged from three measurements and plotted as a function of total solute concentration for each R value studied. The new measurements differed from our original experimental values and agreed with predicted values from both theoretical models. Additionally, the data were fit to the polynomial described in our previous report and the resulting equation was obtained:

$$T_m = (0.383 - 2.145 \times 10^{-3}R)x + (8.119 \times 10^{-3} - 2.909 \times 10^{-5}R)x^2$$

where x is the total solute mass-fraction. This new equation provided good fits to the experimental data as well as published values and relates the determined polynomial constants to the R value of the corresponding isopleths of the three dimensional phase diagram, allowing the liquidus curve for any R value to be obtained.

Keywords: cryobiology, ethylene glycol, phase diagram, calorimetry

Introduction

Currently, many cells and tissues are cryopreserved by dissolving a cryoprotective agent (CPA) in a physiological salt solution for cryopreservation processing. The result of this is the creation of a mixture of water, the CPA, and isotonic salt. Ordinarily, the primary extracellular osmolyte is NaCl, at a concentration

*Corresponding author

Email address: Erik@gnrlbiotech.com (Erik J. Woods)

5 of about 0.90 mass-fraction. During equilibrium freezing of this binary mixture, pure water is trapped as ice, leaving the residual solution enriched with salt. Adding CPA to this mixture increases cryosurvival through its effective dilution of these residual salts, and thereby potentially mitigating “solution effects” injury [8].

In particular, the addition of a CPA to a solution of water and salt has three primary influences on the crystallization process. The initial composition determines the path of crystallization toward a particular crystalline mixture which is in equilibrium at low temperatures, determines the liquidus temperature, and determines the system’s viscosity at a given temperature. In order to understand and optimize the beneficial effects of the dilution of this residual solution by the addition of a CPA, a knowledge of the liquidus surface of the ternary system H₂O-NaCl-CPA is needed.

Several different groups have previously studied phase diagrams for various ternary systems including water, sodium chloride and a CPA [1, 5, 6, 7, 13, 14, 16]. Typically this is achieved by determining melting points as a function of solute concentration for several values of the CPA to NaCl ratio R . Because only water is crystallized during equilibrium freezing protocols, such mixtures behave as a binary mixture because the ratio R does not change during freezing until the eutectic is reached. The resulting curves, or isoplethal sections (essentially vertical planar cuts through the three-dimensional phase diagram), can be described using a polynomial in R and mass-fraction x to relate the determined polynomial coefficients to the R value of the corresponding isopleth. This ultimately allows determination of an equation describing the liquidus curve for any R value of the ternary system, and therefore the ability to identify the melting point corresponding to any total solute concentration or the total and individual solute concentrations corresponding to any temperature, assuming equilibrium cooling rates.

While experimental determination of ternary solutions is cryobiologically important, it can also be expensive and time consuming. Recently, methods to synthesize ternary phase diagrams from binary phase diagram data have been proposed, and synthesized curves have been in close agreement with many known measured results [2, 6], with the exception of the data set from our previous study investigating the system H₂O-NaCl-ethylene glycol [16]. For these reasons, the present study was performed to re-evaluate this system using updated methods and equipment including a differential scanning calorimeter (DSC) to measure melting points (T_m) of solutions with five different R values. A polynomial was then developed to characterize the liquidus surface to generate curves for any R value. The final objective was to compare the resulting experimental data and polynomial fit with the Kleinhans and Mazur binary solution freezing point summation method [6] and the thermodynamically based virial equation method of Elliott et al. [2]—recently applied by Elmoazzen et al. [3] and recently reviewed by Prickett et al. [12]—which is similar but includes additional terms related to solute interactions.

Materials and Methods

The solutions used in this study consisted of NaCl, ethylene glycol (99.5 and 99% pure, respectively; Sigma Aldrich¹, St Louis, MO) and cell culture water (Cellgro, Mediatech, Inc., Manassas, VA, U.S.A) prepared by weight to obtain final R values of 5, 10, 15, 30, and 45. Melting curves for the R values were determined by measuring three levels of concentration within each R . A DSC (Perkin Elmer Corp., Norwalk CT) was set up for sub-ambient operation using liquid nitrogen. The DSC provided thermograms based on a signal proportional to the difference between the heat input to the reference and the heat input to the sample (the actual temperatures of both were equal throughout, however the sample pan heat input deviated from the reference during exo- or endothermic reactions). In experiments of this nature, a thermal lag may result between the temperature of the holding pan and that of the sample. By using a small sample and a slow heating rate, this was minimized, and although variations in thermal lag affect the DSC thermogram peak shape, the peak area remains unchanged (this is in contrast to the DTA technique, where variations in thermal lag do affect peak area and instrument sensitivity is proportional to its value). Due to the relatively high concentration of the ethylene glycol involved in the experimental design, the leading edge slope of the melting curves is technically difficult to measure. Therefore, to obtain the most accurate melting point, Pyris Software (Perkin Elmer Corp., Norwalk CT) was used to determine offset temperatures of the melting endotherm: the point at which the ending edge slope intersected the scanning base line was considered to corresponded closest to the true T_m . The accuracy of the measurement was tested by comparing the developed NaCl-water binary phase diagram with the published data and less than 5% relative difference was observed.

Prior to the experimental runs, a two point calibration was performed using pure indium (Perkin Elmer Corp., Norwalk CT) and highly purified water. After calibrating, standards were re-measured to determine an error estimate (± 0.2 °C as a standard deviation for water and indium; $n = 5$).

An aliquot of each sample (3-5 mg) was deposited into a volatile aluminum sample pan which was then hermetically sealed. Each pan was loaded into the device at and allowed to equilibrate to 5 °C. To obtain the melting endotherm, the samples were cooled at 10 °C/min to -150 °C and held there for 1 minutes to allow equilibration prior to warming. Warming proceeded at 5 °C/min to 5 °C, and during this time the thermogram was taken.

Classically, multi-component equilibrium phase diagrams have been constructed by measuring the melting point of a sample of combinations of components. These data are points on the liquidus surface, and a functional relationship is usually described after the data are collected relating component concentrations

¹The mention of specific products, trademarks, or brand names is for purposes of identification only. Such mention is not to be interpreted in any way as an endorsement or certification of such products or brands by the National Institute of Standards and Technology. All trademarks mentioned herein belong to their respective owners.

to melting points. In Cryobiological literature, the form of these equations has been either quadratic in nature ([13, 10], or fully nonlinear [11, 4]. While the accuracy and efficacy of using this post-hoc method of functional description is sufficient for each set of components, it is unwieldy to implement for systems involving more than three components. Because of this two groups independently have proposed methods whereby multi-component phase diagrams could be constructed only with knowledge of the binary phase diagrams for each of the solutes [12, 3, 6, 2].

Both models use quadratic or cubic equations in molality as the basis of their binary phase diagram models. This polynomial expansion is described in thermodynamics as the osmotic virial equation (cite: your favorite physical chemistry textbook), and can be thought of a second or third order MacLauren approximation of the osmolality with molality m as the variable. To relate freezing point depression to osmolality, we follow the arguments of Prickett et al. who derive the relationship between the freezing point depression $\Delta T_{FP} := T_{FP}^0 - T_{FP}$ and the solution osmolality π

$$\frac{\Delta T_{FP}}{T_{FP}^0 - \Delta T_{FP}} = \frac{W_1 R}{s_1^{0L} - s_1^{0s}} \pi, \quad (1)$$

where $W_1 = 1.802 \times 10^{-2}$ kg/mol is the molecular weight of water, $T_{FP}^0 = 273.15$ is the melting point of pure water, $R = 8.314$ J/mol K is the universal gas constant, and $\overline{s_1^{0L}} - \overline{s_1^{0s}} = 22.00$ J/mol K is the difference in entropy per mole of pure liquid and solid water. We thus define

$$f(\Delta T_{FP}) := \frac{\Delta T_{FP}}{T_{FP}^0 - \Delta T_{FP}} \frac{\overline{s_1^{0L}} - \overline{s_1^{0s}}}{W_1 R}. \quad (2)$$

Note that clearing fractions in equation (1) and assuming ΔT_{FP} is small yields the equation

$$\Delta T_{FP} \approx 1.86\pi. \quad (3)$$

Finally, note that equation (1) may be solved for

$$\Delta T_{FP} = \frac{RT_{FP}^0 W_1 \pi}{s_1^{0L} - s_1^{0s} + RW_1 \pi} := h(\pi) \quad (4)$$

To implement the osmotic virial approach in this manuscript we will use the nonlinear relationship between osmolality and freezing point depression, fitting

$$f(\Delta T_{FP}) = g(m, A, B, C, \delta) := A\delta m + B(\delta m)^2 + C(\delta m)^3, \quad (5)$$

for solute dependent constants A , B , and C , while holding $A = 1$ constant. When the solute does not dissociate, we fix $\delta = 1$, but for solutes that dissociate such as sodium chloride, we fit for this parameter as well. Finally, Elliott et al. claim that the third virial coefficient may be unnecessary except in the case of highly non-ideal solutes (e.g. macromolecules such as Hemoglobin) noting that fitting highly quadratic data for cubic coefficients induces unnecessary error. We will investigate this claim below.

Elliott et al. derive a multisolute model from thermodynamic theory to support the adding of osmolalities that also includes a solute-solute interaction terms derived from the theory of mixing in gases, yielding a freezing point depression equation that can be determined solely by a priori known osmotic virial coefficients.

95 In order to deal with solutes that dissociate such as salts like NaCl, we use $m_1 = \delta \hat{m}_1$, where δ is a dissociation parameter and \hat{m}_1 is the nominal molality. Elliott et al. argue that δ must be fit along with the virial coefficients. Thus, according to Elliott et al. the solution osmolality with one dissociating and one non-dissociating solute may be written as either

$$g_{\text{virial}_2}(\mathbf{m}, \mathbf{B}, \delta) = \underbrace{(\delta m_1 + B_1(\delta m_1)^2)}_{\text{Added Osmolalities}} + \underbrace{(m_2 + B_2 m_2^2) + (B_1 + B_2)\delta m_1 m_2}_{\text{Mixing term}}, \quad (6)$$

or

$$g_{\text{virial}_3}(\mathbf{m}, \mathbf{B}, \mathbf{C}, \delta) = \underbrace{(\delta m_1 + B_1(\delta m_1)^2 + C_1(\delta m_1)^3)}_{\text{Added Osmolalities}} + \underbrace{(m_2 + B_2 m_2^2 + C_2 m_2^3) + (B_1 + B_2)\delta m_1 m_2 + 3C_1^{2/3} C_2^{1/3}(\delta m_1)^2 m_2 + 3C_1^{1/3} C_2^{2/3} \delta m_1 m_2^2}_{\text{Mixing term}} \quad (7)$$

depending on whether solutes are fit to a quadratic or cubic polynomial. The freezing point depression may then be recovered with $\Delta T_{FP} = h \circ g$.

Kleinhans and Mazur take a simpler approach, fitting the equation

$$\Delta T_{FP} = g(m, A, B, C, \delta), \quad (8)$$

for solute dependent constants A , B , and C , holding $\delta = 1$ constant. In Kleinhans and Mazurs model the osmolalities are simply added, and the nonlinear relationship between osmolality and freezing point depression is absorbed into the parameters A , B and C . Given molalities m_1 and m_2 , and known constants A_i , B_i , and C_i , $i = 1, 2$, the “additive osmolality” freezing point depression equation then is

$$g_{\text{add}}(\mathbf{m}, \mathbf{A}, \mathbf{B}, \mathbf{C}) = (A_1 m_1 + B_1 m_1^2 + C_1 m_1^3) + (A_2 m_2 + B_2 m_2^2 + C_2 m_2^3), \quad (9)$$

where bold faced values indicate vector quantities.

In summary, we fit model (5) or (8) to both the NaCl and Ethylene Glycol binary phase diagrams to determine A , B , C , and δ parameters, respectively in the following cases: for model (9) A , B and C are unconstrained and $\delta = 1$; for model (6) $A = 1$ and $C = 0$ are fixed; and for model (7) $A = 1$ is held constant. 110 For models (6) and (7), δ is held fixed at unity for EG and is fit for in the NaCl case. These coefficients can be used in models (9), (6), and (7) to compare synthesized or predictive models with the data. Binary phase diagram data are published in older editions of the CRC Handbook of Chemistry and Physics [15] and by Melinder [9].

The binary phase diagram data for sodium chloride include 81 data points over a molality ranging 115 from 0 to 4.613 mol/kg. Freezing point depression data are given in 0.1, 0.2, and 0.5% weight fraction

increments from 0–5, 5–10, and 10–15%, respectively, and in 1% increments from 15 to 23%. As pointed out by Kleinhans and Mazur [6] fitting to too many points at the lower concentrations weighs the lower concentrations too heavily. Therefore we weighted the datapoints in the fits according to the weight fraction step size. Published EG data on the other hand, combined from both the CRC Handbook [15] and the Melinder data [9], are much more evenly spaced and as such did not require reduction.

Finally, to provide a polynomial fit of the data unconstrained by theory and more convenient to implement in cryobiological applications where R is constant during equilibrium freezing protocols, the quadratic polynomial

$$T_m = (a_1 + a_2R)x + (b_1 + b_2R)x^2 \quad (10)$$

was fit to experimental data for a_i and b_i , $i = 1, 2$, and the coefficient of determination R^2 was calculated for all polynomial models.

All regressions were performed using the Mathematica NonLinearModelFit function (Wolfram Research, Inc., Mathematica, Version 7.0, Champaign, IL (2008)) set to minimize the sum of squared errors. In the case of the sodium chloride binary fits, we used the Weights option set to the corresponding mass fraction step size for each data point.

Results and Discussion

The quadratic and cubic fits from model (5) to existing binary phase diagrams are shown in Fig. 1, and the resulting values for the coefficients A , B , C and δ are given in Table 1.

The quality of fit is related to the number of fitting parameters, but R^2 values were all greater than 0.997, indicating excellent agreement with the data. Our full fit, corresponding to the techniques described by Kleinhans and Mazur produced nearly identical values for the EG parameters, and slightly different values for the sodium chloride parameters. This difference may be due to slightly different sets of data, but plotting their published function and our fit side by side produced indistinguishable plots (data not shown), indicating that the model is relatively insensitive to parameters as long as the parameters are allowed to be fit freely. Osmotic virial coefficients for EG and NaCl were published by Prickett et al. [12]. Their values for B_{EG} and C_{EG} were 0.037 and -0.001, respectively, which are within the standard error of the mean from the current study.

The experimental results did not agree with our previously measured values. These new measured melting points were plotted as a function of total solute concentration for each R value studied (Fig. 2). These data were then fit simultaneously and the resulting equation

$$T_m = (0.383 - 2.145 \times 10^{-3}R)x + (8.119 \times 10^{-3} - 2.909 \times 10^{-5}R)x^2 \quad (11)$$

was obtained, where x is the total solute mass fraction. This new equation relates the determined polynomial constants to the R value of the corresponding isopleths of the three dimensional phase diagram, allowing the

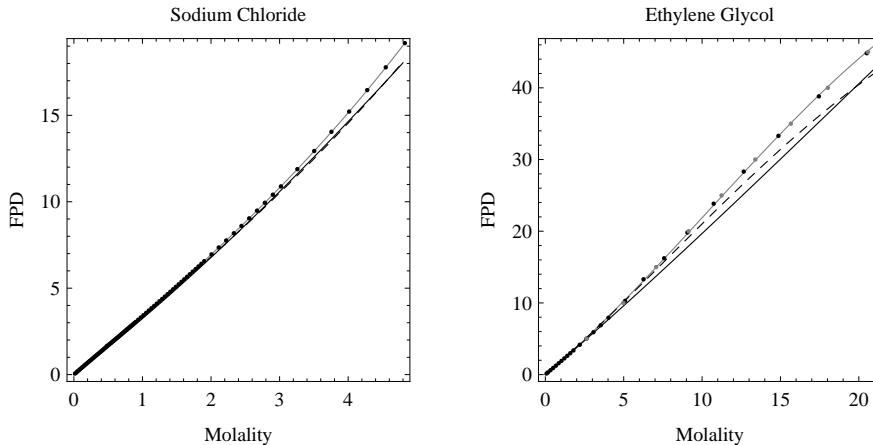


Figure 1: Fits of three models to binary freezing point depression as a function of molality data. The gray, black, and dashed lines indicate curves fitted to the Kleinmans and Mazur formalism, the cubic virial and the quadratic virial, respectively. The sodium chloride data were sourced from [15], and the ethylene glycol data were sourced from both the [15] and [9], with data indicated in black and gray points, respectively.

liquidus curve for any R value to be obtained. The coefficient of determination for the model in display (11) was $R^2 = 0.998$, indicating very good agreement between the model and the data. A similar cubic model produces a better fit, but at the cost of added complexity. Because the quadratic model (11) captured most of the behavior, we chose to publish this one. In contrast, the old model was

$$T_m = (-0.676 + 4.77 \times 10^{-3}R)x + (7.64 \times 10^{-3} + 2.75 \times 10^{-5}R)x^2, \quad (12)$$

and it can be seen from Fig 2 that this old model over-predicts the freezing point depression consistently.

Curves generated using the ternary additive osmolality and osmotic virial models for the same R values are also shown in Fig. 2. Interestingly the synthesized models, and especially the virial models, under-predicted the freezing point depression at higher ethylene glycol concentrations. This is expected because the virial binary fits for EG in Fig. 1 also under-predict the data. This suggests that forcing the first term, A , to be unitary may not be appropriate for EG, though the physical chemical reasons for this is beyond the scope of this manuscript. Both cubic models were virtually indistinguishable, and the quadratic virial model had the poorest predictive values, probably due to the underprediction of the EG binary phase diagram. However, all three synthesized models were within several degrees Celsius of the measured data.

Contrary to our original measurements, which seemed to be skewed towards $R = 0$ these data seem to more closely follow the expected trend as R increases. The resulting curves were very similar to both theoretical models considered. These data seem to support the use of these theoretically constructed phase diagrams based on binary solution freeze point depression data. The two theoretical models also seemed to be in close agreement with each other, however a consistent divergence seems to occur as solute concentration

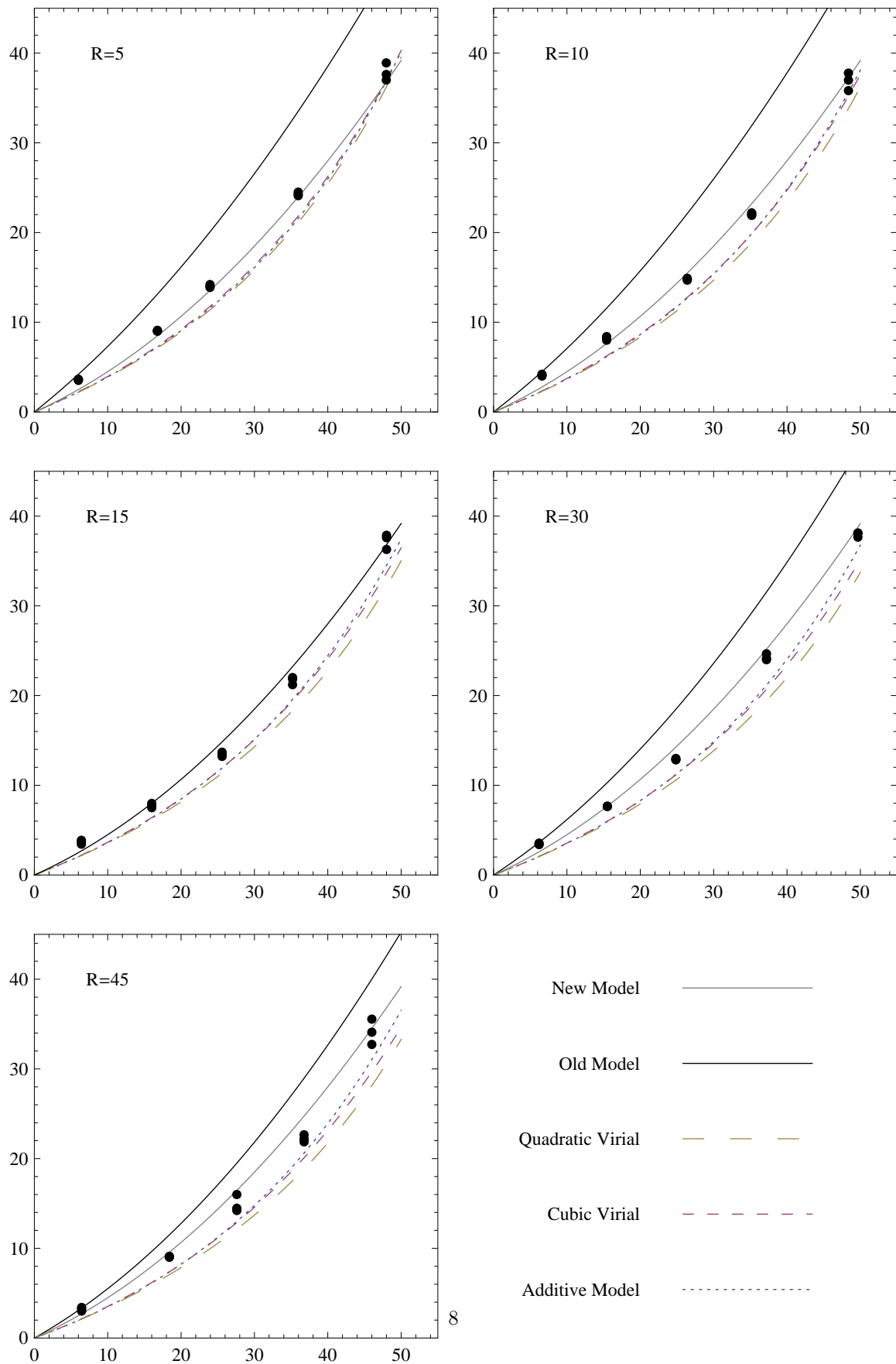


Figure 2: All experimental data points and model predictions at five CPA to sodium chloride ratios. Total mass fraction is given on the horizontal axis and degrees of freezing point depression is given on the vertical axis. The “old model” is the best fit previously published [16], and the “new model” is the best fit to model (11).

Table 1: Coefficients and coefficient of determination for three polynomial model fits to sodium chloride and ethylene glycol binary freezing point depression data. The coefficient of determination, R^2 was greater than 0.997 for all fits.

Solute	A \pm (95% CI)	B \pm (95% CI)	C \pm (95% CI)	$\delta \pm$ (95% CI)
EG ^a	1.8263 \pm 0.0310	0.0534 \pm 0.0043	-0.0017 \pm 0.0001	-
EG ^b	1	0.0310 \pm 0.0007	-0.0008 \pm 0.0001	-
EG ^c	1	0.0140 \pm 0.0012	-	-
NaCl ^a	3.3424 \pm 0.0058	0.0148 \pm 0.004	0.024 \pm 0.0005	-
NaCl ^b	1	0.0041 \pm 0.0006	0.0023 \pm 0.0001	1.7980 \pm 0.0029
NaCl ^c	1	0.0382 \pm 0.0018	-	1.6578 \pm 0.0134

^aAdditive synthesis ^bCubic Osmotic Virial ^cQuadratic Osmotic Virial

165 increases.

Acknowledgements

Research funding for J. Benson was provided by the National Institute of Standards and Technology and a National Research Postdoctoral Associateship.

- 170 [1] Cocks, F., Brower, W., Aug 1974. Phase diagram relationships in cryobiology. *Cryobiology* 11 (4), 340–58, journal Article United states.
- [2] Elliott, J., Prickett, R., Elmoazzen, H., Porter, K., McGann, L., Feb 2007. A multisolute osmotic virial equation for solutions of interest in biology. *Journal of Physical Chemistry B* 111 (7), 1775–1785.
- [3] Elmoazzen, H. Y., Elliott, J. A. W., McGann, L. E., Apr 2009. Osmotic transport across cell membranes in nondilute solutions: a new nondilute solute transport equation. *Biophys J* 96 (7), 2559–71.
- 175 [4] Fahy, G., Nov 1980. Analysis of "solution effects" injury. equations for calculating phase diagram information for the ternary systems nacl-dimethylsulfoxide-water and nacl-glycerol-water. *Biophys J* 32 (2), 837–50.
- [5] Gayle, F., Cocks, F. H., Shepard, M. L., Feb 1977. The H2O-NaCl-Sucrose phase diagram and applications in cryobiology. *Journal of Applied Chemistry and Biotechnology* 27, 599–607.
- [6] Kleinhans, F., Mazur, P., Apr 2007. Comparison of actual vs. synthesized ternary phase diagrams for solutes of cryobiological interest. *Cryobiology* 54 (2), 212–222.
- 180 [7] Liu, J., Gao, D., He, L., Moey, L., Hua, K., Liu, Z., Feb 2003. The phase diagram for the ternary system propylene glycol-sodium chloride-water and their application to platelet cryopreservation. *Zhongguo Shi Yan Xue Ye Xue Za Zhi* 11 (1), 92–5, journal Article China.
- [8] Mazur, P., May 1970. Cryobiology: the freezing of biological systems. *Science* 168 (934), 939–49, 0036-8075 Journal Article.
- 185 [9] Melinder, A., 1997. Thermophysical properties of liquid secondary refrigerants (*EG melting point data communicated to the authors by F. Kleinhans*). Tech. rep.
URL <http://www.mrc-eng.com/news.htm>
- [10] Pegg, D. E., Feb 1983. Simple equations for obtaining melting points and eutectic temperatures for the ternary system glycerol/sodium chloride/water. *CryoLetters* 4, 259–269.

- 190 [11] Pegg, D. E., Feb 1986. Simple equations for obtaining melting points and eutectic temperatures for the ternary system
dimethyl sulfoxide/sodium chloride/water. *CryoLetters* 7, 387–394.
- [12] Prickett, R. C., Elliott, J. A. W., McGann, L. E., Feb 2010. Application of the osmotic virial equation in cryobiology.
Cryobiology 60 (1), 30–42.
- 195 [13] Shalaev, E., Franks, F., May 1995. Equilibrium phase-diagram of the water-sucrose-NaCl system. *Thermochimica Acta*
255, 49–61, ra042 Times Cited:12 Cited References Count:11.
- [14] Shepard, M., Goldston, C., Cocks, F., Feb 1976. The H₂O-NaCl-glycerol phase diagram and its application in cryobiology.
Cryobiology 13 (1), 9–23, journal Article United states.
- [15] Weast, Robert, C, Astle, M. J. (Eds.), 1981. *CRC Handbook of chemistry and physics*. CRC Press, Boca Raton, Florida.
- 200 [16] Woods, E., Zieger, M., Gao, D., Critser, J., Jun 1999. Equations for obtaining melting points for the ternary system
ethylene glycol/sodium chloride/water and their application to cryopreservation. *Cryobiology* 38 (4), 403–7, 0011-2240
Journal Article.